

NONLINEAR ANALYSIS OF THE END ZONES OF PRESTRESSED CONCRETE GIRDERS

Kizzy Van Meirvenne, Department of structural engineering, Ghent University, Belgium

Wouter De Corte, PhD, Department of structural engineering, Ghent University,
Belgium

Veerle Boel, PhD, Department of structural engineering, Ghent University, Belgium

Luc Taerwe, PhD, Department of structural engineering, Ghent University, Belgium

ABSTRACT

Pretensioned concrete girders have been used for many years in construction. Nevertheless, optimization is still possible, especially regarding the anchorage zones. These are typically subjected to different types of stresses due to the local transmission of the prestressing force. By using a 3D nonlinear finite element model, the stresses and cracks in the anchorage zone due to the prestressing forces can be predicted in a more reliable manner. In this paper two 3D FE models are developed by using the concrete damage plasticity model in Abaqus. In the first model, the load transfer is defined by introducing shear stresses around each strand. In the second model, the interaction between the strands and the concrete is introduced by using surface-to-surface contact elements with friction. Finally, to validate the models, the results are compared with strain measurements on a precast beam during production at a precast concrete plant.

Keywords:

Pretensioned Girders, End Zones, FEM, Abaqus

INTRODUCTION

Pretensioned concrete girders have been used for many years in construction.

Nevertheless, there is a lack of unified and practical guidelines for the calculation of the reinforcement in the anchorage zones. The current guidelines as the Eurocode [1], fib Model Code [2], ACI [3] and AASHTOO [4], make use of simplified linear analytical calculation methods or strut-and-tie models. However, only nonlinear models predict the stresses and crack formation in a more reliable manner. Okumus [5] demonstrates this by comparing linear and nonlinear FE calculations of a precast prestressed bridge girder. The two models behave in a similar way until the concrete elements reach their theoretical tensile strength. Once cracking in the concrete occurs, a redistribution of stresses takes place and the rebars become active. The linear models largely underestimate the strains in the concrete, since these models do not consider the stiffness loss of concrete upon cracking.

In this paper a nonlinear FEA is used to assess whether crack formation will or will not occur. FEM is also used to analyze the stress distribution in the girder end zones after prestress release. Two different ways of modeling the prestress transfer, based on respectively Okumus et al. [5] and Abdelatif et al. [6] are implemented and compared with DEMEC measurements on a full-size girder in a precast concrete plant.

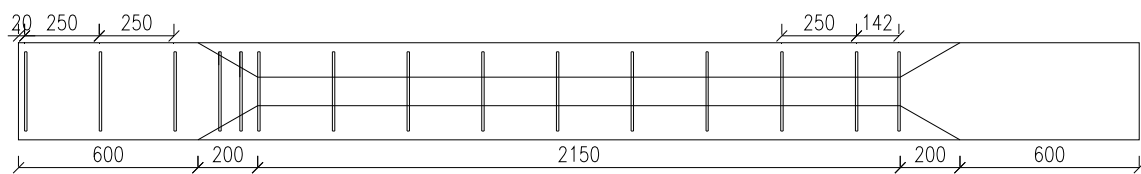
LITARATURE OVERVIEW

Although end zones of precast pretensioned girders have been examined for many years, only recently a growing number of researchers attempts to analyze these zones with nonlinear finite element models. Okumus et al. [5] investigate the end zones of prestressed concrete bridge girders by the use of a nonlinear concrete model. They modeled I-shaped girders using the concrete damaged plasticity (CDP) model in the region with a distance equal to the girder depth from the end of the girder. The prestress force was applied by modeling the strands as gaps in the concrete and applying a tangential surface stress along the strand surface over the transfer length. The applied shear stress was distributed in two different ways, linear and uniform, and the first distribution is concluded to be acceptable, Although the Hoyer effect is not taken in account, the model can be seen as an acceptable simplification. In contrast to Okumus [5], Arab et al.[7] attempted to model the strand as a physical element. They also work with the concrete damaged plasticity model in Abaqus, but the strands are modeled by two different methods, the embedded technique and the extrusion technique. In the first technique, the strands are modeled by 1D-truss elements and are assumed to be embedded in the concrete, which is modeled by solid elements. Although this model seems to contain a feasible methodology and has less computational cost, the methodology renders fewer details regarding the interface between the strands and the concrete, such as the slip and the transfer length. In the extrusion technique the interaction between the strand and the concrete is defined using surface-to-surface elements. Furthermore, normal and tangential behavior properties between the concrete and the strand as the coefficient of friction μ and 'hard' contact are defined. The 'hard' contact is mathematically enhanced by the Lagrange multiplier technique. The modeling approaches are verified based on selected experimental data of Akhnoukh [8]. This way of modeling the end zone of prestressed girders seems to be an appropriate method, not only based on the results of Arab's work, but also on the work of Abdelatif et al. [6]. Abdelatif et al. [6] also make use of the concrete damage plasticity model, although they use the software package Ansys instead of Abaqus. In that work, they did not only present a 3D nonlinear finite element model with interaction between strand and concrete but they also proposed an analytical model based on the thick-walled cylinder theory. Moreover the impact of the

diameter of the prestressing steel, the concrete cover, the concrete strength, the initial prestress and many other parameters are examined in a parametric study. It is noteworthy to mention that both authors propose different values for the coefficient of friction. Abdelatif et al. [6] uses a value of 0.4, whereas Arab et al. [7] prescribes a coefficient of friction between 0.7 and 1.4. In 2015, Yapar et al. [9] propose the most recent attempt to develop a 3D finite element model for a prestressed concrete girder. A comparison between results obtained by numerical modeling and by an experimental 4-point bending test was performed. Deformations as well as crack formations were compared and led to corresponding results. However, it is remarkable that the strands are modeled using an equivalent rectangular cross sections. The aim of the model was not to investigate the transfer of the stresses from the pretensioned strand to the concrete in particular, but to investigate the global behavior after the prestressed girder has been loaded. For this reason, the modeling method of the strands by Arab et al.[7] (extrusion technique) and Abdelatif et al. [6] seems to be the most useful method to model and analyze the end zone. Both models are however applied with only one strand in a concrete rectangular section. The study of this paper is based on the same modeling principles but is applied on the anchorage zone of a full-size girder with multiple strands and compared with the results of the same girder produced at a precast concrete plant. As mentioned before, not only the strand modeling method suggested by Abdelatif et al. [6] will be used but also the simplified method of Okumus et al. [5].

EXPERIMENTAL TEST

In order to validate the finite element models, an experimental test is carried out at a concrete precast plant during regular production. The test girder consists of an I-shaped cross-section with a height of 600 mm (23.62 in), a width of 325 mm (12.80 in) and pretensioned by 10 strands in cross section. In figure 1, 12 strands are indicated but 2 strands (marked with a hatch) are debonded over the full length of the girder. Both girder ends were equipped with an end block with a length of 600 mm (23.62 in). In addition, a transition zone of 200 mm (7.87 in) is provided between the I-shaped cross section and the end block. A sketch of the geometry is presented in figure 1.



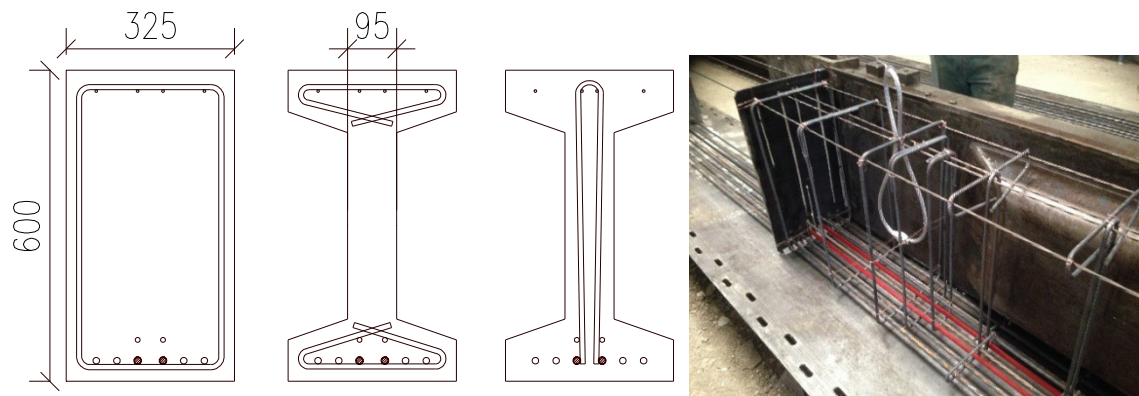


Fig. 1 Geometry of the test girder [mm]

The end zones of the girder are both reinforced in a different way. The right hand side on figure 1, also the active side of the beam (positioned closest to the point of release), is produced without reinforcement. The other side, on the contrary, is produced with a minimum reinforcement consisting of three rectangular stirrups with a diameter of 8 mm (0.31 in) every 250 mm (9.84 in), followed by, in the transmission zone, two rectangular stirrups with the same diameter but with a smaller width. Subsequently, in the I-shaped cross section, I-shaped stirrups with a diameter of 8 mm were installed every 250 mm (9.84 in). In this way, two different configurations could be tested on the same beam. Moreover, in the cross section of the girder three different types of strands are present, each tensioned at a different force as summarized in table 1. The position of the strands remains constant over the full length of the girder.

Table. 1 characteristics of the strands

Strand	Diameter [mm]	A_p [mm ²]/ [in ²]	f_{pk} [N/mm ²]/ [ksi]	Prestress force [kN]/ [kipf]
5 mm	5,2 (0.20")	13,6 / 0.02	1960 / 284.3	21,3 / 4.8
3/8"	9,3	52 / 0.08	1860 / 269.8	77,4 / 17.4
1/2"	12,5	93 / 0.14	1860 / 269.8	138,4 / 31.1

The girder is cast with a self-compacting concrete of grade C55/67 as specified in the European standard [1]. After three days the prestressing strands are released. At the plant, three compression tests were carried out at three days and three tests at 21 days. The results of the cubes of 150x150x150 mm (5.9 in) at 21 days, stored under water at a temperature of 20°C, were recalculated to 28 days using the fib Model Code formulas (1-6) [2]. The compressive strength of the cubes at 21 days was 69.2, 68.0 and 62.1 N/mm² (10.0, 9.9, 9.0 ksi) respectively, resulting in an average of 66.4 N/mm² (9.6 ksi). This average is used to calculate the concrete compressive (f_{cm}) and tensile strength (f_{ctm}) at 28 days and subsequently at three days. With a value of 0.20 for the s-factor, the concrete tensile strength and the compressive strength after three days are calculated as $f_{ctm} = 2.56$ N/mm² (0.37 ksi) and $f_{cm} = 51.8$ N/mm² (7.51 ksi). The latter results are used as input parameters for the concrete damaged plasticity model. Instead of the recalculated values of 21 days to three days, the experimental value of three days may also be used. However, this will not be discussed in this paper.

t	age of the concrete [days]
s	coefficient which depends on the strength class
$f_{ctm}(t)$	mean concrete tensile strength at t days [MPa]
f_{ctm}	mean concrete tensile strength at 28 days [MPa]
f_{ck}	characteristic value of f_c at 28 days [MPa]
f_{ccubm}	Mean cube compressive concrete strength [MPa]

In order to measure the strains in the end zones, several measuring points were attached to the end block's lateral faces with a non-shrinkable adhesive, as presented in figure 2. With an 100 mm (3.9 in) long invar reference bar, provided with two conical locating points, the measurement points were placed at a fixed distance of 100 mm (3.9 in). Near the end face of the beam the measuring points were placed in overlay, with an intermediate distance of 50 mm (2.0 in) in order to obtain more accurate results near the beam end. In the vertical direction, the reference points starts at a distance of 50 mm (2.0 in) of the bottom of the girder and in the horizontal direction at 25 mm (1.0 in) from the end face of the girder. The exact distance between the reference points was then measured with a DEMEC mechanical strain gauge with a basis of 100 mm (3.9 in) and a 16 microstrain resolution. The distance is measured before and after the prestress release. In this way the strains can be calculated at different locations.



Fig. 2 Measurement locations

The results of the horizontal measurements of the reinforced end zone are shown in figure 3. From these, only the results at a level of 50 and 100 mm (2.0 and 3.9 in) from the

bottom of the girder will be compared with the 3D finite element models.

Fig. 3 Measured strains at the end zone

FINITE ELEMENT MODELS

MATERIAL MODELS

Concrete

The concrete material parameters are based on the concrete damage plasticity model as used in Abaqus [10]. This model is appropriate for simulating the nonlinear behavior of concrete in compression as well as in tension. The CDP model is based on the Drucker-Prager hypothesis. An overview of the used input parameters of the concrete model are given in Table 2.

Table. 2 Material properties of concrete

Density ρ [kg/m ³]	2500
Poisson ratio ν_s [-]	0.2
Dilatation angle [°]	30
Eccentricity [mm]	0.1
f_{b0}/f_{c0} [-]	1.16
K [-]	0.666

Beside the general material properties, the CDP model requires several specific input parameters. These define the compressive and the tensile behavior, respectively. The compressive behavior was modeled as a combination of experimental results and theoretical formulas. Figure 4 demonstrates the used CDP with on the left hand side the compression input parameters and the two figures on the right hand side represent the tensile behavior.

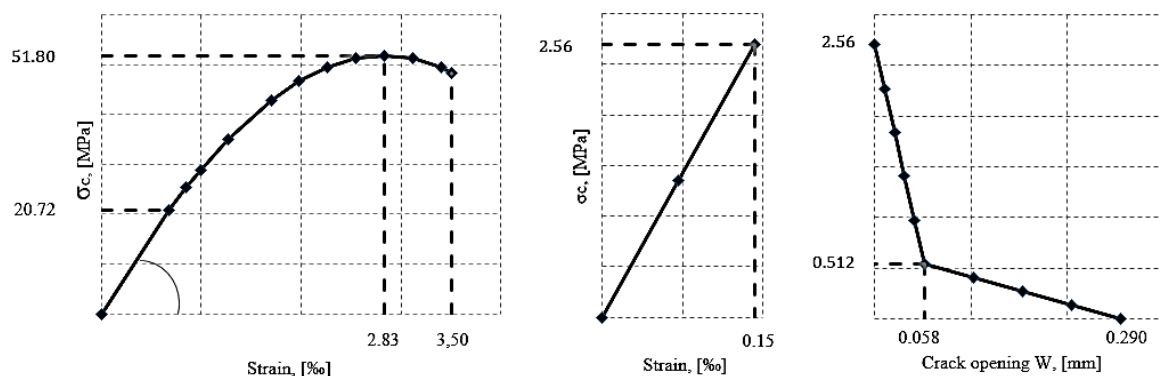


Fig. 4 Used concrete damaged plasticity model

Steel

The steel was modeled as a linear material. Because the stress in the pretensioning steel is always lower than the yield stress, the linear material properties are justified. The calculation model requires the input of several material properties as the volumetric density, the modulus of elasticity and the Poisson ratio. These characteristics are listed in table 3. Both for the stirrup reinforcement as for the prestressing strands the same properties were used.

Table. 3 Material properties of steel

Density ρ [kg/m ³]	7800
Modulus of elasticity E_s [MPa]	200000
Poisson ratio ν_s [-]	0.3

GENERAL MODEL

The modeled girder consists of 3 different parts: the end block (1), the I-shaped girder (2) and the transition element (3) which are all tied together (see figure 5). In each part circular cut-outs were provided at the positions of the strands. Due to symmetry, only one fourth of the beam needs to be modeled (see figure 6). This reduces the computing time and the calculation memory in a significant manner.

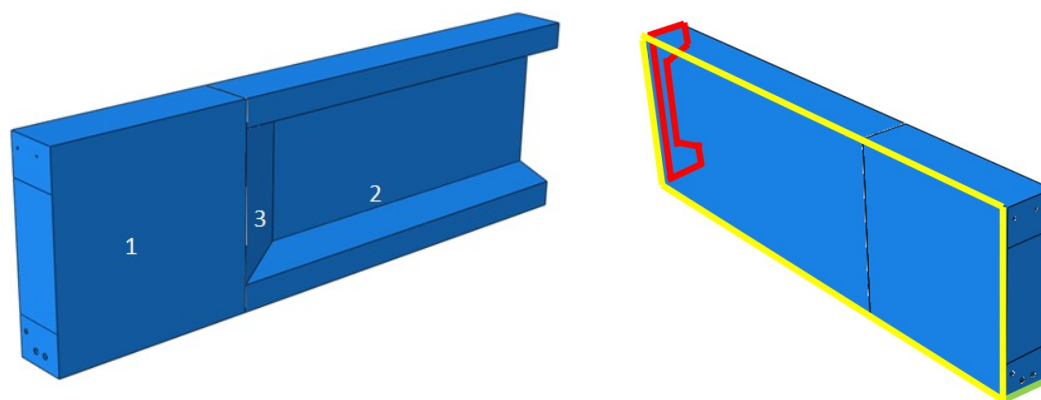


Fig. 5 Geometry of the modeled girder

In order to be able to calculate the stresses, the girder is meshed into small 3D elements. Since the largest stress gradients occur at the end of the beam, the girder is meshed more densely at the girder end and the mesh size is gradually increased away from the girder end, which is shown in figure 7. For the concrete beam hexagonal elements (C3D8R, 8-node linear brick elements with reduced integration) are used whereas for the strands, wedge type elements (C3D6, 6-node linear triangular prism elements) are selected. The quadratic element type would require a larger computation time and results only in a negligible improvement in accuracy.

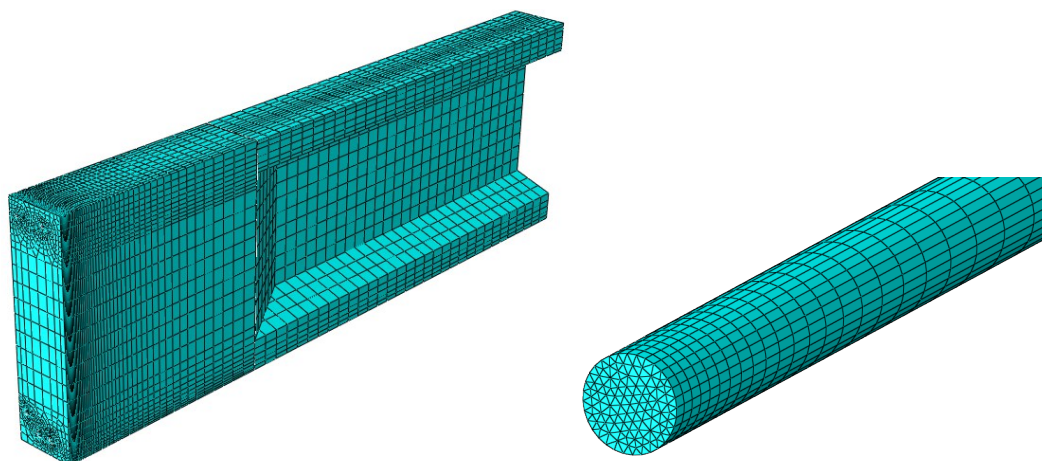


Fig. 7 Mesh of the girder and the strand

LOAD TRANSFER

As mentioned in the literature overview, two different ways of load transfer are modeled. Both methods will be clarified in the next part.

- Classic shear based model

In this way of modeling the load transfer is defined as a shear stress along the strand surface over the transfer length. In this model, the strands are tied to the surrounding concrete. The transfer length is a widely discussed topic in literature [12]. Many researchers examined this length and different formulas are developed which results in a wide scatter on the values [13]. In this paper it is opted to consider the transfer length which is calculated applying the formula of the fib Model Code [11,12]. The transfer length calculated in this way as well as a 50% larger transfer length are modeled. The reason for doing so, is the large range of transfer length as explained before. The transfer length according to the fib Model Code [11] is calculated by equation 7.

$$(7)$$

where α is a value which takes into account the method of the force transfer, and a gradual force transfer results in a value of 1. For the parameter β a value of 0.5 is proposed in the case strands are used. Moreover, A_p is the cross-sectional area of the tendon, ϕ is the nominal diameter of the tendon and σ_s is the steel stress just after release which is considered as $0.7 f_{pk}$, with f_{pk} is the characteristic value of the tensile strength of the prestressing steel assumed as 1860 N/mm² (269.8 ksi) for the 1/2" strand, 1960 N/mm² (284.3 ksi) for the 3/8" strand, and the 5 mm (0.2 in) strands. Parameter γ takes the type of the prestressing tendons into account. The fib Model Code 2010 [11] proposes the value of 1.2 for a 7-wire strand. The position of the tendons is taken into account by δ , where for horizontal tendons a value of 1 is prescribed. The obtained transfer lengths are given in Error: Reference source not found4.

Table. 4 Transfer Length according to fib Model Code 2010 [11]

	1/2 " (12.5 mm)	3/8 " (9.3 mm)	5 mm (5.2 mm / 2.0 in)
--	--------------------	-------------------	---------------------------

Transfer length [mm] / [in]	502.0 / 19.8	377.0 / 14.8	175.8 / 6.9
Transfer length [mm] / [in] + 50%	753.0 / 29.6	565.5 / 22.3	263.6 / 10.4

In order to model the shear stress along the strand, an analytical field is defined in Abaqus. An analytical field defines spatially varying values for selected properties, loads, interactions, and predefined fields, such as the variation of a shear stress over a region [10]. The shear stress is calculated by dividing the prestress force by the perimeter of the strand and the transfer length. Three different models are developed for each strand type. Firstly, a linearly decreasing function towards zero over the transfer length is considered. Secondly, a similar linearly decreasing function reaching zero at a length which is 50% larger is used. The third function is a bilinear function with a maximum at 20% of the transfer length. The first and last mentioned functions are shown in figure 8. As Okumus et al. [5] concluded that a uniform stress distribution is less realistic to model the shear stress, this model is not considered in this paper.

Fig. 8 Functions which define the shear stress along the transfer length

➤ Model with friction

In the second configuration the stress in the strands is modeled as a predefined field. Predefined fields are time-dependent, non-solution-dependent fields that exist over the spatial domain of the model [10]. This corresponds with strands which are first prestensioned and thereafter covered in concrete. Since there were three different strands each with another prestressing force, three separate fields are specified. The interaction between the concrete and the prestressing strands is defined in the longitudinal and radial direction. In the longitudinal direction the Coulomb friction law was used to define the frictional behavior, and the most important parameter to be specified is the coefficient of friction. For the latter parameter different values were taken into consideration. In the radial direction a “hard contact” needs to be chosen. This default pressure-over closure relationship used by Abaqus implies that the surfaces transmit no contact pressure unless the nodes of the slave surface have contact with the master surface. There is no penetration allowed at each constraint location as well as no limit to the magnitude of contact pressure that can be transmitted when the surfaces are in contact [10]. Furthermore, the Augmented Lagrange algorithm was set active. In a last stage, the interaction is defined as a surface-to-surface contact.

Because of the large number of material parameters a lot of scatter of the results is possible. An extensive parametric study, as Abdelatif et al. [6] did for a model with one strand, is highly recommended. In this paper, one of the most important parameters, the coefficient of friction, is studied.

COMPARISON OF EXPERIMENTAL AND FEM RESULTS

Firstly the results of the experimental test at a height of 50 mm (2.0 in) (figure 9) and 100 mm (3.9 in) (figure 10) from the bottom of the beam are compared with the results of the shear transfer based and friction based models. As mentioned, the latter model is calculated with different coefficients of friction. From the first graph it can be seen that

the linear and bilinear results constitute an upper strain limit. Furthermore, the results of the linear model with a 50% larger transfer length and the friction based models with a coefficient of friction between 0.8 and 1.2 have a curve shape similar to the experimental curve, whereas, the models with a lower value for the coefficient of friction have a rather different shape.

Fig. 9 Experimental and analytical results of the strains at 50 mm from the bottom of the girder

In figure 10, an identical trend can be observed. In this figure the linear model is once more represented by the upper limit of strains. Furthermore, the models with a coefficient between 0.8 and 1.2 have a similar shape as the model with a 50% larger transfer length. It must be noticed that in this situation the experimental values have a lower position compared to the analytical values.

Fig. 10 Experimental and analytical results of the strains at 100 mm from the bottom of the girder

It can be questioned whether a different slope would result in similar transversal stresses which lead to cracks in the end face of the girder. In order to solve this question two steps were taken into consideration. In the first step, the transfer lengths of the friction based models were investigated. In the second step, the vertical stresses were calculated in the finite element models.

The transfer length is measured by investigating the longitudinal stresses at the edge of the strand. This length can be estimated at the intersection of a horizontal line at 95% of the maximum stress. According to the results from a 1/2" strand, shown in figure 11, it can be concluded that a higher coefficient of friction results in a lower transfer length. Figure 11 illustrates also the fact that there is no linear relationship between the transfer length and the coefficient of friction.

Fig. 11 Transfer length with a varying coefficient of friction

In a next step, the vertical stresses are measured in each model at a certain level over approximately 150 mm (5.9 in) from the end of the girder. In this way the occurring vertical splitting force, which leads to cracks in the end zones, can be calculated. Figure 12 depicts that vertical stresses at the concrete surface are calculated at a height of 250 mm (9.8 in) and 300 mm (11.8 in) counted from the bottom of the beam, because at these levels the largest area with the highest vertical stresses is present. The tensile stress

distribution along the mentioned height of 250 mm (9.8 in) is displayed in figure 13.

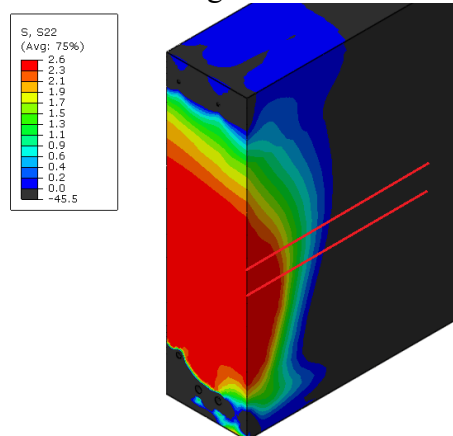


Fig. 12 Location of the calculated vertical stresses **Fig. 13** Vertical stresses at 250 mm [N/mm²]

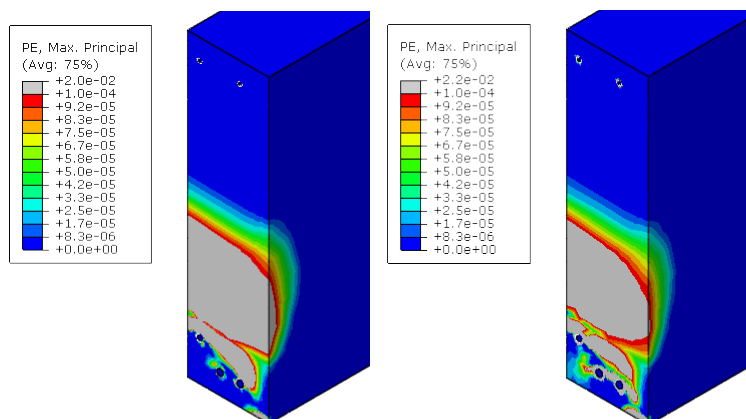
Subsequently, the vertical splitting force can be calculated by making the sum of, the integral of the vertical concrete stress multiplied by the width of the beam, and the forces in the modeled reinforcement. At the earlier mentioned levels of 250 and 300 mm (9.8 and 11.8 in), the forces are calculated for the different models and they are summarized in table 5. For the shear based models two values for the transfer length are given in the table, the first one is the modeled length and the second one is 95% of this length. When analyzing the values in the table, it can be seen that it is indeed correct to assume that the linear shear based model results in the largest vertical splitting force. This linear shear based model emerges also as the upper bound in figure 9 and 10. In these figures, the shear based model with the larger transfer length is most similar to the friction based models with a coefficient between 0.8 and 1. Depending on the level where the vertical stresses are determined, different values can be found.

Table. 5 Calculated splitting force at a height of 250 mm and 300 mm

	L _{bpt} (left, center) and 95% L _{bpt} (right) [mm] / [in]		Vertical Force in concrete 250 mm [kN] / [kipf]	Force in the rebars [kN] / [kipf]	Total Force 250 mm [kN] / [kipf]	Vertical Force 300 mm [kN] / [kipf]	Total Force 300 mm [kN] / [kipf]
MC linear	502 / 19.7	476.9 / 18.8	83.5 / 18.8	3.4 / 0.8	86.9 / 19.5	84.6 / 19.0	88.0 / 19.8
MC bilinear	502 / 19.7	476.9 / 18.8	84.9 / 19.1	3.3 / 0.7	88.2 / 19.8	84.5 / 19.0	87.8 / 19.7
MC lin.+50%	753 / 29.6	715.4 / 28.2	77.3 / 17.4	2.4 / 0.5	79.7 / 17.9	76.4 / 17.2	78.8 / 17.7
μ = 0.6	722.6 / 28.4		59.5 / 13.4	2.1 / 0.5	61.7 / 13.9	60.2 / 13.5	62.3 / 14.0
μ = 0.7	627.6 / 24.7		64.2 / 14.4	2.4 / 0.5	66.7 / 15.0	65.5 / 14.7	67.9 / 15.3
μ = 0.8	557.5 / 21.9		69.4 / 15.6	2.7 / 0.6	72.1 / 16.2	71.2 / 16.0	73.9 / 16.6
μ = 0.9	513.5 / 20.2		72.6 / 16.3	2.8 / 0.6	75.4 / 17.0	74.6 / 16.8	77.4 / 17.4
μ = 1.0	476.8 / 18.8		75.7 / 17.0	3.0 / 0.7	78.7 / 17.7	77.9 / 17.5	80.9 / 18.2
μ = 1.1	447.4 / 17.6		78.0 / 17.5	3.1 / 0.7	81.2 / 18.3	80.3 / 18.1	83.5 / 18.8
μ = 1.2	431.9 / 17.0		79.0 / 17.8	3.2 / 0.7	82.2 / 18.5	81.5 / 18.3	84.8 / 19.1

This is the reason why the vertical forces for these particular models were calculated at different levels spacing 5 mm (0.2 in), starting from the bottom of the beam. Because it is not certain whether the level where the area of the highest value is presents, also results in the largest vertical splitting force. The results of this calculation show that the maximum value of the shear based model with a 50% larger transfer length (MC lin. +50%) is 80.5 kN (18.1 kipf)calculated at a height of 275 mm (10.8 in). For the friction based models the maximum values are 73.9 kN, 77.5 kN and 81.1 kN (16.6, 17.4 and 18.2 kipf) for the coefficients of friction 0.8, 0.9 and 1 respectively. This implies that the spalling force of the shear based model is 0.7% smaller and 3.7% larger than the friction based models with the coefficient of 0.9 and 1 respectively. These results suggest that both models predict the spalling force in a similar way. However, it is noteworthy that the transfer lengths are not equally long. This is due to the fact that the transfer length is defined differently. In the first model, the transfer length is the length started from the end face of the girder until the point where the shear stress is zero (figure 8). In the second model, on the contrary, the transfer length is estimated at the intersection of a horizontal line at 95% of the maximal stress in the strand. This stress is lower than the initially modeled stress in the predefined field. For example, on the 1/2” strand a predefined stress of 1128 N/mm² (163.6 ksi) was applied while the maximum measured stress in the strand is 1029 N/mm² (149.2 ksi). This means that it is highly probable that the model takes prestress losses into account.

As a last part of the comparison between the experimental and analytical data, the plastic strain, which is an indication of the damaged zone, is investigated. In the earlier mentioned results, the linear model shows the highest spalling force followed by the model with a coefficient of friction of 1.2. The same result can be observed in figure 14, because a larger spalling force results in a larger damaged zone. To be complete, the linear model with the larger transfer length is also taken into consideration. However during, and shortly after, the experimental test, no cracks occurred. Due to the presence of the transition zone, the strains could not be measured over a sufficiently long length of the end zone of the girder. As such, in order to calculate the most feasible transfer length or coefficient of friction, the DEMEC measurements in this case cannot lead to a decisive conclusion.



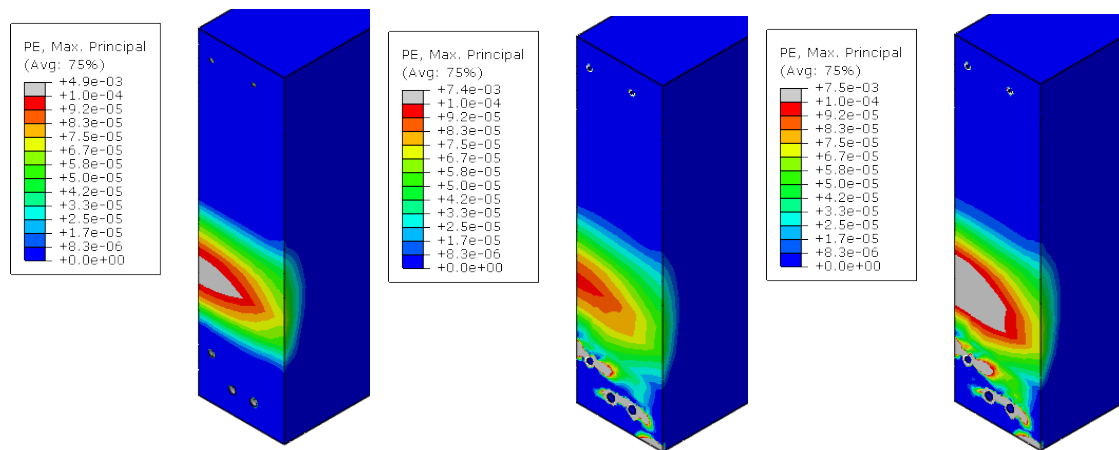


Fig. 14 Results of the plastic strain

DISCUSSION AND CONCLUSION

This paper starts with experimental tests on a full size girder in a precast concrete plant. The tests consist of DEMEC measurements on the side of the girder. This is followed by modeling the load transfer in two different ways, namely shear and friction based. The first model is based on the work of Okumus et al. [5] where no rectangular end zone was considered. Okumus et al. [5] modeled an I-shaped end zone whereas in this work a rectangular zone is modeled. For the second model the principles are based on the work of Abdelatif et al. [6]. In the present study the model is extended with multiple strands. Out of the comparison between the experimental and analytical models, two preliminary conclusions can be taken.

Firstly, the results of the linear model with a 50% larger transfer length, as calculated by the fib Model Code, and the friction based models with a coefficient of friction between 0.8 and 1.2 have a similar curved shape. This is also reflected in the results for the calculated spalling force and the size of the plastic strain areas. These findings are a first validation which leads to promising results and prove that both modeling techniques can be used. Unfortunately, these modeling techniques cannot yet be generalized to all the possible prestressed girders. A second experimental girder will bring more clarity about the transfer length and the correct value for the coefficient of friction. However, a first promising attempt is certainly made.

A second conclusion can be made regarding the results of the linear shear based model and the model with a coefficient of friction of 1.2. The first mentioned model is the upper limit in the results. This is also reflected in the results because it has the highest values for the spalling force and the plastic strain area. These values are similar to the results of the model with the coefficient of friction of 1.2, which is the nearest graph to the linear shear based model. In order to create design formulations for calculating the reinforcement in the end zones, these input parameters can be used to quantify the reinforcement area in a secure manner. The reinforcement will probably be over dimensioned but it will be a safe approach. Here again, a second validation is needed prior to using these parameters.

As a main conclusion, these results suggest that the two different ways of modeling gives a similar result, although, the shear based model is a simplified model and does not take the Hoyer effect into account. It is proven that an extended friction based model with

multiple strands can be designed and leads to comparable results with the experimental test. Regarding the optimization of the end zone, this was not yet investigated in literature. Unfortunately, both models have an unknown factor. The transfer length in the first model and the coefficient of friction in the second model. The value for this latter parameter is in this work assumed to be in a range of 0.8 to 1.2, where in literature various values are found. However, defining the value for this parameter out of one experiment would be too premature. A next and comprehensive experimental test will bring definite answers in this promising research.

ACKNOWLEDGMENTS

This research was supported by the Agency for Innovation by Science and Technology (IWT) and the company Structo+, producers of reinforced and prestressed beams, columns, floor elements, roof elements and bridge girders. The authors wish to express their gratitude for the support.

REFERENCES

1. CEN. Eurocode 2: design of concrete structures – Part 1–1: general rules and rules for buildings. European standard EN 1992-1-1:2004: Brussels: Comité Européen de Normalisation, 2004.
2. Comité-Euro-International du Béton, Model Code 2010, Lausanne: fib, 2011.
3. ACI Committee 318. Building code requirements for reinforced concrete (ACI 318-11). Farmington Hills, MI: American Concrete Institute, 2011.
4. American Association of State Highway and Transportation Officials, AASHTO LRFD 2012 Bridge Design Specifications, (6), pp. 5-168 - 5-169, 2012.
5. Okumus P, Oliva and Becker, “Nonlinear finite element modeling of cracking at ends of pretensioned bridge girders.” *Engineering Structures* 40, pp. 267-275, 2012.
6. Abdelatif J, Owen and Hussein, “Modeling the prestress transfer in pre-tensioned concrete elements,” *Finite Elements in Analysis and Design*, pp. 47-63, 2015.
7. Arab A, Badie and Manzari, “A methodological approach for finite element modeling of pretensioned concrete members at the release of pretensioning,” *Engineering Structures*, 33 (1918-1929), 2011.
8. Akhnoukh AK, “Development of high performance precast/prestressed bridge girders. Doctoral dissertation.” Department of Civil Engineering. University of Nebraska-Lincoln, 2008.
9. Yapar O, Basu and Nordendale, “Accurate finite element modeling of pretensioned prestressed concrete beams,” *Engineering Structures*, pp. 163-178, 2015.

10. Dassault Systèmes Simulia Corporations, Abaqus analysis user's manual, Providence: Simulia, 2012.
11. FIB. Model Code 2010. First complete draft. Fib Bulletin No. 55, vol. 1. Lausanne: International Federation for Structural Concrete, 2010.
12. Martí-Vargas J.R., Serna, Navarro-Gregori, Pallarés, “Bond of 13 mm prestressing steel strands in pretensioned concrete members.” *Engineering Structures* 41, pp.403–412, 2012.
13. Van Meirvenne K, De Corte, Boel, Taerwe, “Numerical and experimental analysis of the transfer length and its influence on the anchorage zone design of pretensioned concrete.” CTU congress, Dundee 2016.